DATA SUPPLEMENT

Atrial-selective targeting of arrhythmogenic phase-3 early afterdepolarizations in human myocytes

S. Morotti[1], A.D. McCulloch[2], D.M. Bers[1], A.G. Edwards[3,4], E. Grandi[1,@]

[1] Department of Pharmacology, University of California Davis, Davis, CA, USA
[2] Department of Bioengineering, University of California San Diego, La Jolla, CA, USA
[3] Institute for Experimental Medicine, Oslo University Hospital Ullevål, Oslo, Norway
[4] Simula Research Laboratory, Lysaker, Norway

Table S1 – EADs occurrence at varying model parameters (□ No EAD, ■ EAD).

	-5%	-3%	+3%	+5%
G_{Na}		■	■	■
G_{Ca}	■	■	■	■
$I_{NCX,max}$	■	■	■	■
$I_{NaK,max}$	■	■	■	■
G_{Nab}	■	■	■	■
G_{Cab}	■	■	■	■
$I_{PMCA,max}$	■	■	■	■
G_{RyR}	■	■	■	■
SERCA V_{max}	■	■	■	■
G_{to}	■	■	■	■
G_{Kur}	■	■	■	■
G_{Kr}	■	■	■	■
G_{Ks}	■	■	■	■
G_{K1}	■	■	■	■
G_{Kp}	■	■	■	■
G_{Cl}	■	■	■	■
G_{ClCa}	■	■	■	■

G_{Na}, Na^+ current conductance; G_{Ca}, L-type Ca^+ current conductance; $I_{NCX,max}$, Na^+/Ca^{2+} exchanger maximal transport rate; $I_{NaK,max}$, Na^+/K^+ pump maximal transport rate; G_{Nab}, Na^+ background current conductance; G_{Cab}, Ca^{2+} background current conductance; $I_{PMCA,max}$, sarcolemmal Ca^{2+} pump maximal transport rate; G_{RyR}, ryanodine receptors conductance; SERCA V_{max}, SERCA maximal transport rate; G_{to}, transient outward K^+ current conductance; G_{Kur}, ultra-rapid delayed rectifier outward K^+ current conductance; G_{Kr}, rapidly activating delayed rectifier K^+ current conductance; G_{Ks}, slowly activating delayed rectifier K^+ current conductance; G_{K1}, time-independent K^+ current conductance; G_{Kp}, plateau K^+ current conductance; G_{Cl}, background Cl^- current conductance; G_{ClCa}, Ca^{2+}-dependent Cl^- current conductance.

@ Department of Pharmacology, University of California Davis, 451 Health Sciences Drive, GBSF rm 3502, Davis, CA 95616, USA
E-mail: ele.grandi@gmail.com Phone: (530) 752-4334 Fax: (530) 752-7710

Equilibrium *vs*. non-equilibrium components of I_{Na}

We characterized total and theoretically maximum equilibrium components of the Na^+ current (I_{Na}) observed during repolarization of three different repolarization ramps (50-, 100-, and 500-ms long, Fig. S1A).

To do this, we plotted total simulated I_{Na} (Fig. S1B), which at any time is the sum of late (I_{NaL}), non-equilibrium ($I_{Na,NE}$), and equilibrium ($I_{Na,win}$) currents:

$$I_{Na} = I_{Na,win} + I_{Na,NE} + I_{NaL}$$

and calculated the maximum steady-state window current ($I_{Na,win,max}$, Fig. S1C) that would eventually occur at each instantaneous E_m during repolarization using E_m-dependence of steady-state activation & inactivation (SSA & SSI, MS Fig. 4B-C):

$$I_{Na,win,max} = G_{Na,max} \cdot SSI \cdot SSA \cdot \left(E_m - E_{Na}\right)$$

These calculations show that total I_{Na} during rapid repolarization ramps (Fig. S1B black/red traces) is already substantial at E_m (and times) where $I_{Na,win,max}$ is virtually absent (Fig. S1C black/red traces). This indicates that some non-equilibrium (dynamic) component is responsible for this E_m-dependence, and therefore for the majority of the I_{Na} during the simulated rapid repolarization. Also, as observed in Edwards *et al* [1], slower repolarization reduces total I_{Na}, despite the theoretically steady-state $I_{Na,win,max}$ being trajectory-independent (only depends on instantaneous E_m). During this very gradual repolarization, total I_{Na} reaches at most 5% of that during rapid repolarization at any region of the voltage range (Fig. S1D, inset). Importantly the E_m-dependence of the very small current elicited during the slowest ramp is much more similar to that of $I_{Na,win,max}$ (Fig. S1D, blue line in inset *vs*. black dashed line), suggesting that the window current contributes much more purely to this current.

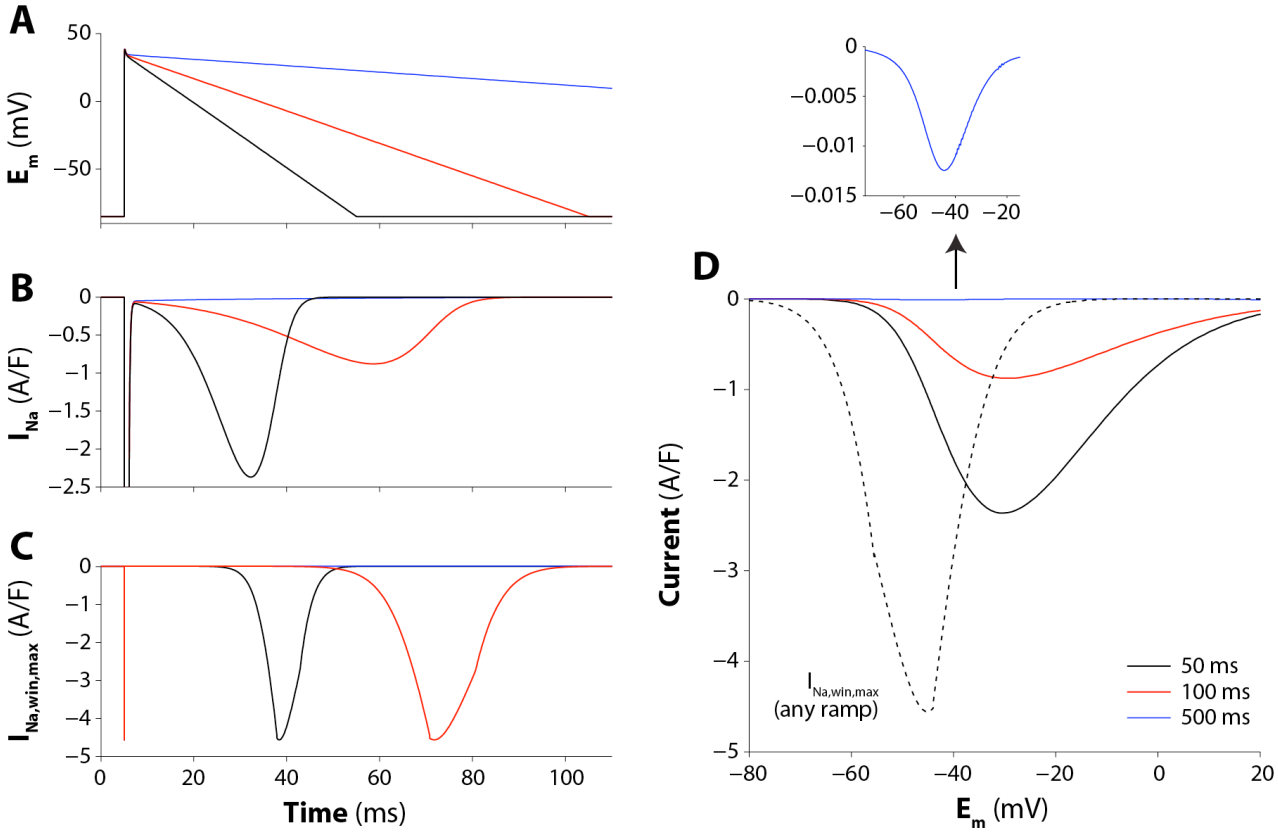

Figure S1. A) 50-(black) 100-(red) and 500-ms (blue) long repolarizing ramps used as voltage commands. **B)** Simulated I_{Na} and **C)** theoretical maximal window current elicited by the voltage waveforms in (**A**). **D)** Instantaneous I_{Na}- and $I_{Na,win,max}$-voltage curves are calculated from **B** and **C** (repolarization phase only).

Variability in phase-3 EAD morphology

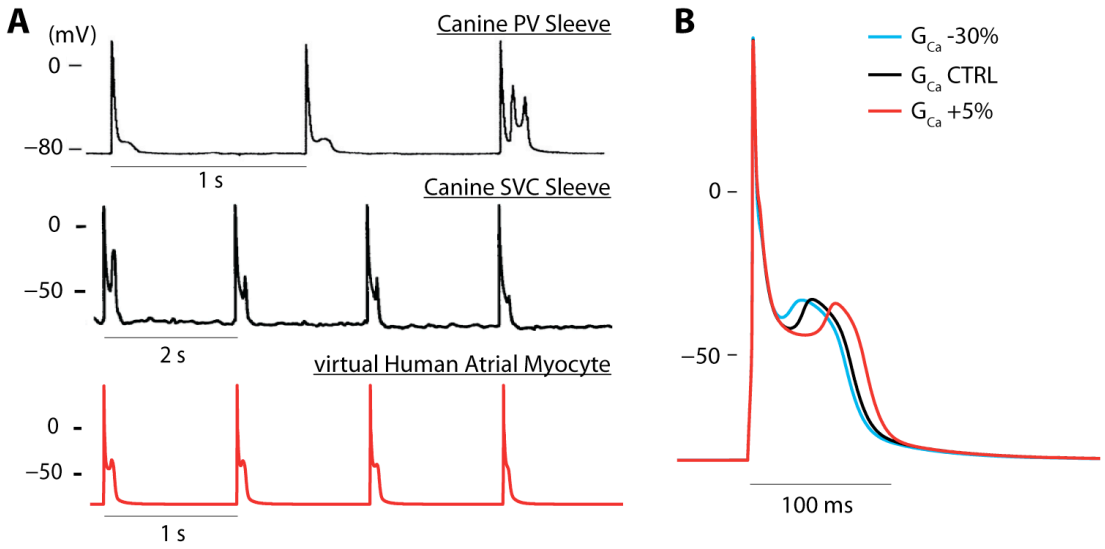

Figure S2. A) ACh- and high Ca^{2+}-induced late phase-3 EADs are observed at slow rates in beats immediately after rapid pacing in both canine PV (reproduced with permission from [2]) and superior vena cava (reproduced with permission from [3]) sleeves. Third row shows EADs evoked in our human atrial model (G_{Ca} +5%) under ACh and ISO conditions. **B)** Effect of varying I_{Ca} conductance on EAD take-off potential.

References

1. Edwards *et al*. Circ Arrhyth Electrophysiol. 2014 Dec; 7(6): 1205–1213
2. Sicouri *et al*. Heart Rhythm. 2008 Jul; 5(7): 1019–1026
3. Sicouri *et al*. Circ Arrhythm Electrophysiol. 2012; 5:371-379